THE JOURNAL OF PHYSICAL CHEMISTRY B

Article

pubs.acs.org/JPCB

Prototropism of [2,2′-Bipyridyl]-3,3′-diol in Albumin−SDS Aggregates

Dipanwita De, Kalyan Santra, and Anindya Datta*

Department of Chemistry, Indian Institute of Technology, Bombay Powai, Mumbai 400 076, India

Supporting Information

ABSTRACT: In this present investigation, attempt is made to use [2,2′-bipyridyl]-3,3′-diol ($BP(OH)_2$) as a marker to study albumin−SDS interactions and to obtain structural information about these aggregates. It is also intended to contemplate the effect of these aggregates on the excited-state proton-transfer dynamics of $BP(OH)_2$. Steady-state and time-resolved fluorescence spectroscopic techniques are employed to elucidate the nature of interaction of two homologous carrier proteins, human serum albumin (HSA) and bovine serum albumin (BSA), with negatively charged surfactant sodium dodecyl sulfate (SDS). Both spectral and temporal behavior of $BP(OH)_2$ in these albumin−SDS aggregates strongly affirm an initial competitive binding of SDS in high-energy binding sites of albumin. Unlike normal SDS micelles, the absence of formation of the monocation of $BP(OH)_2$ at the negatively charged interface of SDS is rationalized by screening of the micellar interface in the presence of denatured protein which wraps around these surfactant aggregates. An enhanced extent of excited-state proton transfer is manifested by a corresponding increase in fluorescence quantum yield of $BP(OH)_2$ in these aggregates. Temporal evolution of $BP(OH)_2$ at different emission wavelengths fortifies the formation of normal micelles post saturation. All our observations are found to corroborate with the necklace and bead model proposed for protein−surfactant aggregates.

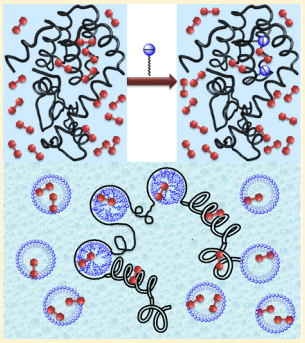

INTRODUCTION

The cooperative binding of anionic ligands with proteins has been a subject of interest for decades due to its biological applications in designing various drug delivery systems.[1−4] Interactions between surfactant and serum albumins are well-established[5,6] as serum albumins serve as the internal delivery vesicles by binding with many biologically activated compounds such as drugs, fatty acids, and steroids and thus carries them to targeted cells. Human serum albumin (HSA) and bovine serum albumin (BSA) are two homologous carrier proteins of blood plasma with a single polypeptide chain of 585 and 583 amino acids, respectively.[7] Though these globular proteins exhibit similar conformation properties, their optical properties are different as BSA contains two tryptophan residues, whereas HSA has one.[8] Furthermore, unlike a single unfolded state in HSA, BSA has two distinct unfolded states in the pH range of 4.8−5.6.[7] This results in a pH-dependent binding of ligand with BSA. In contrast, the effect of pH on fluorescence properties of HSA−ligand complex is absent. HSA has two primary drug binding sites called Sudlow's site I and II located in subdomains IIA and IIIA where drugs like warfarin, dansyl-L-proline, ibuprofen, benzodiazaphene, and aspirin bind.[9] Apart from drugs, surfactants are also known to bind with albumin proteins leading to denaturation.[10] Sodium dodecyl sulfate (SDS), an anionic surfactant, is known to interact strongly with these globular proteins and, thereby, initiates unfolding.[11] The interaction and denaturation process upon binding of SDS with albumin proteins has been previously monitored using fluorescence quenching of intrinsic tryptophans and circular dichroism spectroscopy at pH 5.0, 7.0, and 9.0.[12,13] The surfactant-induced denaturation is reported to have a binding isotherm having four distinct regions.[14] The initial regions are characterized by specific high-energy binding followed by noncooperative interactions. Finally, extensive cooperative binding due to unfolding of the protein occurs, beyond which saturation is attained. Further addition of surfactants leads to the formation of normal micelles. The necklace and bead model has been proposed as the most acceptable structure of protein surfactant aggregate by employing various spectroscopic techniques like fluorescence, NMR, and ESR.[14] In the necklace and bead model the protein envelops around the polar head groups of the surfactant aggregates (Scheme 1). Various probes have been used to mark the interactions within these macromolecular aggregates.[15−17] Turro and Lei[14] used fluorescence of pyrene monomer and excimer to probe BSA−SDS interactions while Vasilescu et al.[18] investigated BSA−CTAB (cationic surfactant), BSA−$C_{12}E_8$ (neutral surfactant), and lysozyme−SDS (anionic surfactant) complexes using pyrene with different quenchers. Fluorescence quenching electron-transfer studies between several 7-amino coumarin dyes and *N*,*N*-dimethylaniline have been used as a tool by Chakraborty et al. to elucidate possible structure of BSA−SDS complexes.[15]

[2,2′-Bipyridyl]-3,3′-diol ($BP(OH)_2$) is a fluorophore known to exhibit excited-state intramolecular double proton transfer (ESIDPT).[19,20] Single-crystal X-ray analysis[21] reveals that the

Received: June 19, 2012
Revised: August 6, 2012
Published: August 22, 2012

Scheme 1. Schematic Representation of the Necklace and Bead Model Where the Protein (Red) Wraps around the Surfactant Aggregates (Blue)

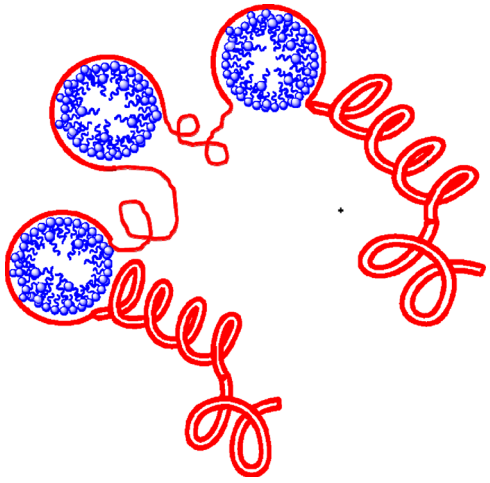

dienol tautomer (DE) of $BP(OH)_2$ has a planar geometry in the ground state with two strong intramolecular hydrogen bonds which exist in all nonaqueous solvents (Scheme 2).[22]

Scheme 2. Chemical Structures of Dfferent Tautomers of $BP(OH)_2$ Formed after Excited-State Proton Transfer

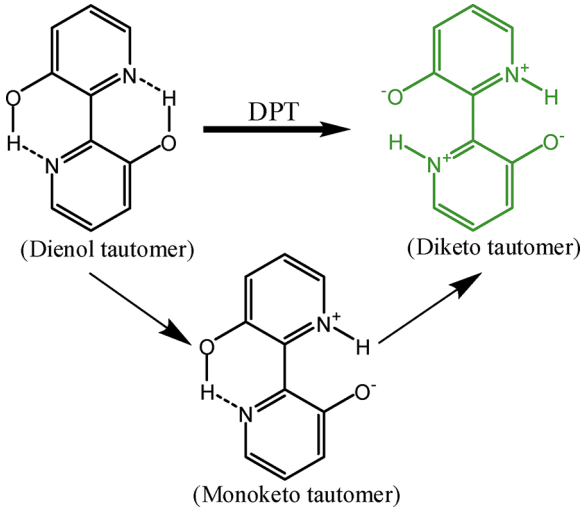

The diketo tautomer (DK) formed after double proton transfer is responsible for the strong green fluorescence observed in $BP(OH)_2$.[22] Femtosecond fluorescence upconversion technique[23] and transient absorption measurements[24] are used to elucidate excited-state photophysics of this probe. The monoketo tautomer (MK) formed during stepwise proton-transfer reaction via single proton transfer has been identified in the excited state with a lifetime of 100 fs with no evidence of its formation in the ground state.[25] The monoketo tautomer thereby formed relaxes to emissive diketo tautomer in ~10 ps.[26] In contrast, the concerted proton-transfer reaction has been reported to be ultrafast (less than 100 fs).[27] Probable applications of $BP(OH)_2$ and its derivatives as dye lasers in inert solvents,[28] molecular half-subtractors,[29] solar energy collectors, and photostabilizers of polymers have been explored.[30]

The photophysics of ESIDPT in $BP(OH)_2$ has been explored to a great extent in both neat solutions[20,22] and organized assemblies like cyclodextrins,[31−33] micelles,[19] zeolites,[34] binary mixtures of *p*-dioxane/water,[35] and HSA.[31] Theoretical[36,37] and electro-optical measurements[38] as well as spectral features in solvents with different polarities support the fact that the dienol and diketo tautomer have a negligible dipole moment due to their C_{2h} symmetry and the MK form has a dipole moment of 4.0−4.9 D. The dienol tautomer of $BP(OH)_2$ absorbs around 350 nm in neat solutions and emits in green with quantum yield varying from 0.2 to 0.4.[22] Though in all nonaqueous solvents the dienol tautomer of $BP(OH)_2$ exists in the ground state, water is reported to show a unique second absorption band between 400 and 430 nm due to the formation of intermolecularly hydrogen-bonded water complexes.[33] The low-energy band in water is due to stabilization of the diketo tautomer in the ground state while the high-energy band is assigned to the lowest $\pi-\pi^*$ transition of the dienol form. pH-dependent photophysics of $BP(OH)_2$ has been studied by Rurack et al., and the four pK_a values have been ascertained as 0.16, 2.69, 9.2 and 12.4.[34] Earlier we have reported the modulation of ESIDPT dynamics of $BP(OH)_2$ in nanocavities of micelles where the negative interface of SDS alters its excited- and ground-state photophysics.[19] As a continuation of this endeavor, an attempt is made to explore the effect of macromolecular interactions between SDS and serum albumins (HSA and BSA) on ESIDPT of $BP(OH)_2$. Binding of $BP(OH)_2$ with HSA has been reported using steady-state measurements.[31] This article reports a detailed time-resolved investigation of the photophysics of $BP(OH)_2$ upon binding with HSA.

MATERIALS AND METHODS

The anionic surfactant, SDS, is purchased from Sigma-Aldrich. HSA (fatty acid and globulin free) is obtained from Sigma. BSA, sodium dihydrogen phosphate (GR), and disodium hydrogen phosphate (GR) are acquired from Merck. $BP(OH)_2$ (98% pure) is from Aldrich. All the compounds are used as obtained without any further purification. Phosphate buffer solutions of pH 5.6 and 7 using Millipore water are used, and an ionic strength of 0.2 is maintained during all measurements. In order to prevent inner filter effect, the absorbance of $BP(OH)_2$ in buffer solution is kept around 0.2 with $BP(OH)_2$ concentration of ≈0.03. Protein−surfactant interactions are studied using 1% protein, and the concentration of SDS is varied from 0 to 100 mM. The fluorescence quantum yields of $BP(OH)_2$ in protein−surfactant aggregates are determined using a quantum yield value of 0.51 for quinine sulfate at 25 °C as a standard.[39] Steady-state spectra are recorded on a Jasco V-530 spectrophotometer and Varian Cary Eclipse spectrofluorimeter. Emission spectra of $BP(OH)_2$ are recorded using excitation wavelengths of 350, 375, and 406 nm. Time-resolved fluorescence measurements are performed in a picosecond pulsed diode laser-based time-correlated single photon counting (TCSPC) instrument from IBH (United Kingdom) set at a magic angle of 54.7°. The excitation source used is 375 nm (laser) with fwhm of 250 ps having a resolution of 7 and 14 ps/channel. The number of channels per decay for 7 and 14 ps/channel resolutions are 8192 and 4096, respectively. The fluorescence decays are fitted using a biexponential model using iterative reconvolution after deconvolution. IBH DAS 6.2 data analysis software[40,41] is used for multiexponential fitting of the decay traces. The error associated with determination of

dx.doi.org/10.1021/jp306027h | J. Phys. Chem. B 2012, 116, 11466−11472

lifetimes for the short component is 0.5−2.5%, and that for the long component is 0.1−1%.

RESULTS AND DISCUSSION

Binding of $BP(OH)_2$ with Proteins. Absorption spectra of $BP(OH)_2$ recorded in buffer (pH 5.6 and pH 7) consist of two distinct bands at 350 and 406 nm as observed in aqueous solution. In presence of 1% (150 μM) albumin proteins (HSA or BSA) there is a small red shift of the 350 nm band while the low-energy band is suppressed to a great extent, indicating destabilization of the diketo form in the hydrophobic environment of protein (Figure 1). Successive increments in

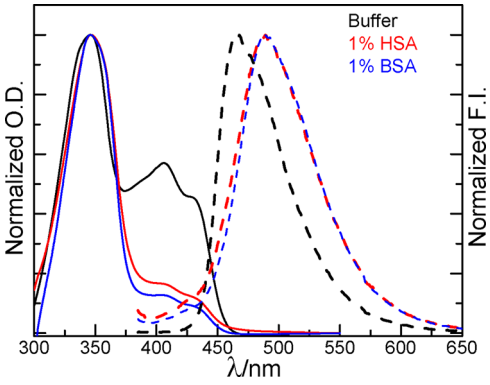

Figure 1. Normalized absorption and emission spectra of $BP(OH)_2$ in buffer (pH 7), 1% HSA, and 1% BSA (λ_{ex} = 375 nm).

HSA concentration from 0 to 150 μM result in an increase in quantum yield of $BP(OH)_2$ with a red-shifted emission band (Figure 2a). Concentrations above 150 μM have not been used, as further red shift in the fluorescence spectrum does not take place beyond this concentration.[31] The 25 nm red-shifted emission spectra in albumin proteins is an outcome of net stabilization attained by the diketo tautomer in the excited state upon binding (Figure 1). This observation is in line with that reported in another work, in recent past,[31] which reports the

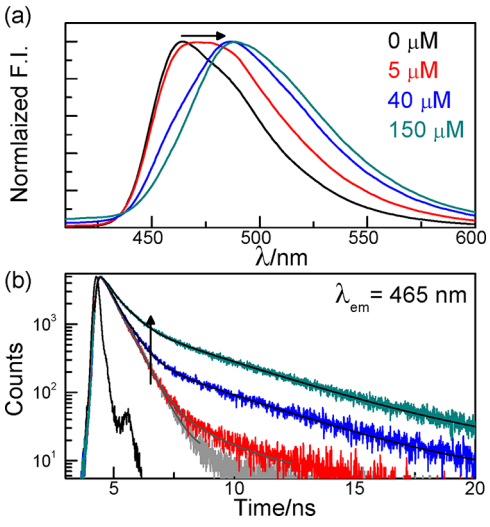

Figure 2. (a) Normalized emission spectra (λ_{ex} = 350 nm) and (b) fluorescence transients (λ_{ex} = 375 nm) of $BP(OH)_2$ in varying concentrations of HSA at pH 7. The fluorescence decays are recorded at emission wavelength of 465 nm. (The increase in HSA concentration from 0 to 150 μM is shown by the arrow.)

expected binding site of $BP(OH)_2$ is located in subdomain IIA of HSA. Time-resolved fluorescence study in buffer (pH 7) shows $BP(OH)_2$ exhibits a decay with a short lifetime of 0.6 ns, which on addition of HSA becomes progressively slower (Figure 2b and Table 1). Though HSA-bound $BP(OH)_2$ has a

Table 1. Time-Resolved Fluorescence Decay Parameters of $BP(OH)_2$ with Varying Concentrations of HSA at λ_{ex} = 375 nm and λ_{em} = 465 nm (pH 7)

[HSA] (μM)	τ_1/ns	A_1	τ_2/ns	A_2	χ^2
0	0.59 ± 0.002	1.0			1.05
5	0.55 ± 0.004	0.98	2.32 ± 0.016	0.02	1.00
40	0.55 ± 0.002	0.96	3.60 ± 0.030	0.06	1.04
150	0.60 ± 0.003	0.83	3.75 ± 0.010	0.17	1.08

characteristic lifetime of around 3.7 ns, the contribution of the short component (0.60 ns) predominates irrespective of emission wavelength, indicating the existence of free probes even at the highest protein concentration used. Hence, one may infer that the diketo excited state is more long-lived within the albumin proteins, most likely by virtue of shielding from water.

Steady-State Spectra of $BP(OH)_2$ in Albumin Protein−SDS Aggregates. The protein−surfactant interaction is studied by gradual addition of SDS to 1% protein solution in buffer of pH 5.6, which is the condition maintained in earlier studies.[14,15] Initial addition of SDS, up to a concentration of 2 mM in 1% protein solution of $BP(OH)_2$, leads to a decrease in absorbance of $BP(OH)_2$ at 350 nm, accompanied by a simultaneous increase in the 406 nm band (Figure 3). This

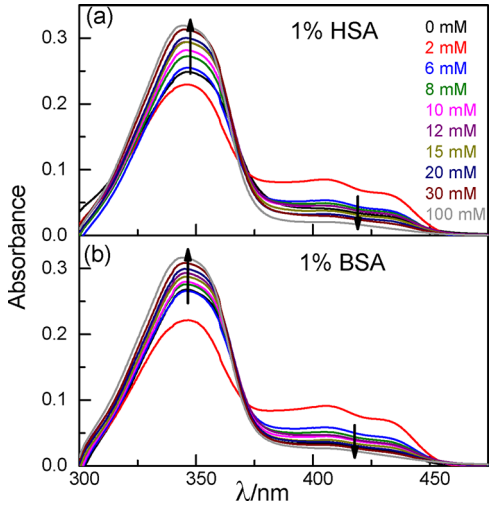

Figure 3. Absorption spectra of $BP(OH)_2$ in 1% HSA (a) and 1% BSA (b) with addition of SDS where the concentration varies from 0 to 100 mM. The arrows indicate increasing concentration of SDS.

observation can be rationalized in terms of early specific binding of SDS at high-energy sites of serum albumins, as reported in literature,[14] leading to an initial compression. This results in release of fluorophore into buffer solution due to competitive binding with SDS, and thus, absorbance at 406 nm becomes prominent. Further addition of SDS augments unfolding of albumins leading to significant cooperative binding between SDS and protein. It may be noted here that SDS is reported[12,13] to denature the secondary structure of albumin proteins. Presence of $BP(OH)_2$ does not affect the con-

dx.doi.org/10.1021/jp306027h | J. Phys. Chem. B 2012, 116, 11466−11472

formation of HSA as affirmed from the circular dichroism spectrum (Figure S1 of the Supporting Information). These macromolecular assemblies encapsulate the fluorophore, resulting in increase of ground-state population of the dienol form, which absorbs at 350 nm, accompanied with gradual decrease in the population of the diketo tautomer, as the fluorophore experiences a more nonpolar environment[32] (Figure 3). Moreover, the presence of an isosbestic point at lower concentration of SDS is a signature of two-state equilibrium between diketo and dienol forms which is disrupted at higher SDS concentration. Such isosbestic point is absent in normal SDS micelles owing to the formation of monocation at the Stern layer with an additional band at 370 nm as observed earlier.[19] However, the spectra at very high SDS concentrations do not pass through the isosbestic point, indicating the formation of normal SDS micelles after saturation of SDS binding with albumin proteins. Therefore, our observations can be explained by the necklace and bead model where the protein wraps around the surfactant aggregates and the negatively charged head groups of the surfactant molecules are not exposed to water.[14,15,42]

The dienol and diketo tautomers absorb around 350 and 406 nm, respectively, as discussed in the previous section. Due to the presence of ground-state heterogeneity emission spectra of $BP(OH)_2$ are monitored at excitation wavelengths of 350, 375, and 406 nm. For all the excitation wavelengths, an increase in fluorescence quantum yield (ϕ_f) of the probe is observed in presence of 1% albumin as compared to buffer solution of pH 5.6 (Figure 4). In the present investigation, SDS concentration

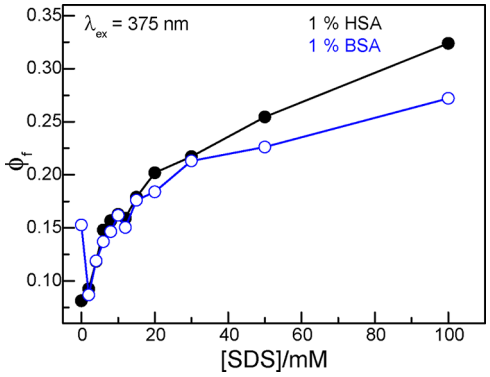

Figure 4. Quantum yield of $BP(OH)_2$ in 1% HSA and 1% BSA as a function of SDS concentration from 0 to 100 mM. (λ_{ex} = 375 nm.)

of 2 mM in 1% protein solution is marked by an initial dip in the fluorescence quantum yield of $BP(OH)_2$ for BSA–SDS, which is in line with previous observations for pyrene and TNS (2-toluidinylnaphthalenesulfonate) used for probing BSA–SDS interaction by Turro and Lei.[14] This reinforces the contention that selective binding of SDS at high-energy sites of these globular proteins competes and, thereby, expels the fluorophores into the aqueous environment. Surfactant-induced unfolding of albumins accompanied by massive binding occurs on further addition of SDS. This is manifested by a marked increase in fluorescence quantum yield (ϕ_f) which is prominent even before the critical micelle concentration (cmc) of SDS is attained (Figure 4). Denaturation followed by coiling of the protein around SDS aggregates further solubilizes $BP(OH)_2$ in an environment that is more hydrophobic than native protein or normal micelles.

The shift of the fluorescence maxima in albumin protein–SDS aggregates follows a complex nature. $BP(OH)_2$ exhibits an emission maximum at 490 nm in 1% albumin solution. Upon addition of SDS, a blue shift is observed until a concentration of 2 mM SDS (Figure 5 and Figures S2 and S3 of the Supporting

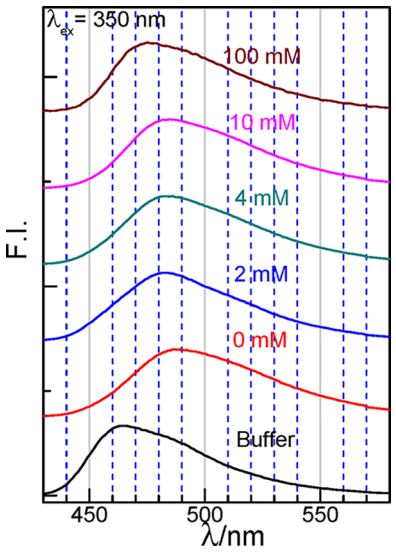

Figure 5. Emission spectra of $BP(OH)_2$ in buffer and 1% HSA with increasing SDS concentrations at excitation wavelength of 350 nm. (The SDS concentrations are 0, 2, 4, 10, and 100 mM as specified in the plot.)

Information). This may be ascribed to the discharge of fluorophores into the aqueous environment due to competitive binding of SDS with proteins. Beyond 2 mM SDS unfolding of protein commences, as is evidenced by a progressively red-shifted emission maxima. This is in accordance with the previous discussion on spectral behavior under the consideration of the "necklace and bead" model. The position of the emission maximum in SDS–protein aggregate is more red-shifted than in normal SDS micelles. This lends credence for the formation of smaller and compact protein-wrapped surfactant aggregates providing greater hydrophobicity to the probe as suggested by Turro and Lei.[14] The formation of normal micelles beyond SDS concentration of 10 mM results in an emission maximum of 475 nm, which is the same as observed earlier in SDS micelles.[19] The observed shift is less prominent for excitation at 406 nm where the diketo tautomer present in the aqueous region absorbs (Figures S2c and S3c of the Supporting Information).

Time-Resolved Fluorescence Studies in Albumin Protein–SDS Aggregates. Fluorescence transients are obtained using pulsed excitation at 375 nm with emission monitored at 465 and 510 nm (Figure 6 and Figure S4 of the Supporting Information). The fluorescence decays are biexponential. $BP(OH)_2$ in buffer solution of pH 5.6 exhibits a faster decay with a short lifetime of 0.6 ns as discussed previously for pH 7. In presence of 1% albumin (HSA or BSA), $BP(OH)_2$ exhibits a long component of around 3.80 ns (τ_2) in addition to 0.60 ns (τ_1), due to binding in the hydrophobic region. The long component of 3.80 ns (τ_2) in albumins is comparable with the lifetime of $BP(OH)_2$ in protein-free SDS micelle as reported previously.[19] Though subsequent addition of SDS in presence of 1% protein does not affect the long lifetime much, the short component increases from 0.60 ns to

dx.doi.org/10.1021/jp306027h | J. Phys. Chem. B 2012, 116, 11466–11472

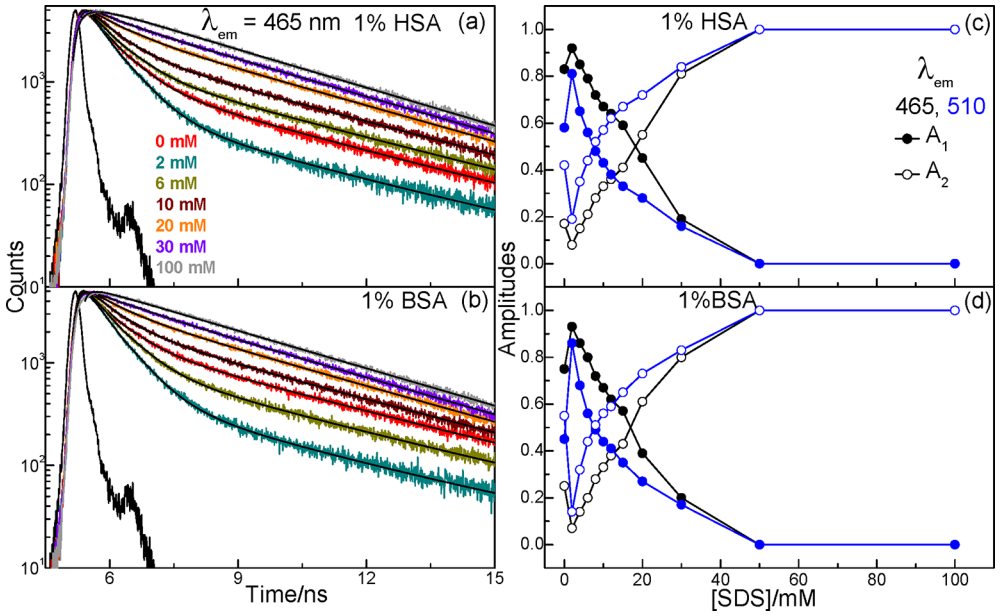

Figure 6. Fluorescence transients of $BP(OH)_2$ in (a) 1% HSA and (b) 1% BSA with increasing SDS concentration at λ_{ex} = 375 nm and λ_{em} = 465 nm (left panel). The concentrations of SDS are specified in the legend. The variation of amplitudes of two components of biexponential fits to the decay traces recorded at two different emission wavelengths (465 and 510 nm) for $BP(OH)_2$ in (c) 1% HSA and (d) 1% BSA as a function of SDS concentration (right panel).

Table 2. Time-Resolved Fluorescence Decay Parameters of 1% Albumin Solution of $BP(OH)_2$ with Varying Concentrations of SDS at λ_{em} = 465 nm

albumin	[SDS] (mM)	τ_1/ns	A_1	τ_2/ns	A_2	χ^2
1% HSA	0	0.60 ± 0.003	0.83	3.75 ± 0.010	0.17	1.08
	2	0.60 ± 0.002	0.92	3.80 ± 0.020	0.08	1.06
	6	0.62 ± 0.003	0.79	3.91 ± 0.010	0.21	1.04
	10	0.66 ± 0.005	0.67	3.85 ± 0.011	0.33	1.01
	20	0.69 ± 0.008	0.45	3.64 ± 0.012	0.55	1.05
	30	0.77 ± 0.006	0.19	3.56 ± 0.010	0.81	1.09
	100			3.53 ± 0.005	1.00	1.12
1% BSA	0	0.62 ± 0.004	0.75	3.88 ± 0.014	0.25	1.02
	2	0.61 ± 0.002	0.93	3.72 ± 0.032	0.07	1.03
	6	0.63 ± 0.004	0.80	3.94 ± 0.022	0.20	1.10
	10	0.70 ± 0.005	0.67	3.88 ± 0.012	0.33	1.07
	20	0.74 ± 0.008	0.39	3.62 ± 0.012	0.61	1.11
	30	0.86 ± 0.007	0.20	3.54 ± 0.026	0.80	1.12
	100			3.54 ± 0.004	1.00	1.15

around 0.85 ns depending on the emission wavelength (Table 2 and Table S1 of the Supporting Information). The monocation of $BP(OH)_2$ formed in the interfacial region of the Stern layer in SDS is known to exhibit a radiative lifetime of 1 ns.[19] The formation of monocation is ruled out in albumin−SDS aggregates because of the presence of an isosbestic point and absence of an additional shoulder in absorption spectra as discussion in the previous section. Thus, the increase in lifetime of the short component provides an evidence of trapping of the probe in interfacial water of these macromolecular aggregates which retards excited-state dynamics.

The variation of the amplitudes (A_1 and A_2) of the two radiative lifetimes has an interesting trend (Figure 6, parts c and d). The shorter component shows appreciably high contribution in presence of 1% proteins at both the blue and red edge of the fluorescence spectrum. Initially, at 2 mM SDS the contribution of the shorter lifetime increases significantly accentuating the release of some fluorophore into the hydrophilic region upon competitive binding. As the concentration of SDS is increased further, the contribution of the short component decreases owing to SDS-induced unfolding of albumins. A subsequent increase in the contribution of long radiative lifetime is observed as a function of SDS concentration. Finally, the decay transients become single-exponential with a long lifetime of around 3.5 ns above 30 mM SDS due to incorporation of the probe in SDS−albumin aggregates and normal SDS micelles. At a particular SDS concentration, the decay recorded at the red edge is slower than that of the blue edge due to greater contribution of $BP(OH)_2$ bound to these aggregates (Figure 7). The difference in the decays disappears gradually indicating absence of free probe in water. Thus, the temporal evolution of $BP(OH)_2$ in presence of protein−surfactant aggregates is in line with steady-state measurements. The spectral and temporal behavior of the fluorophore endorses the "necklace and bead model" proposed for protein−surfactant aggregates.

dx.doi.org/10.1021/jp306027h | J. Phys. Chem. B 2012, 116, 11466−11472

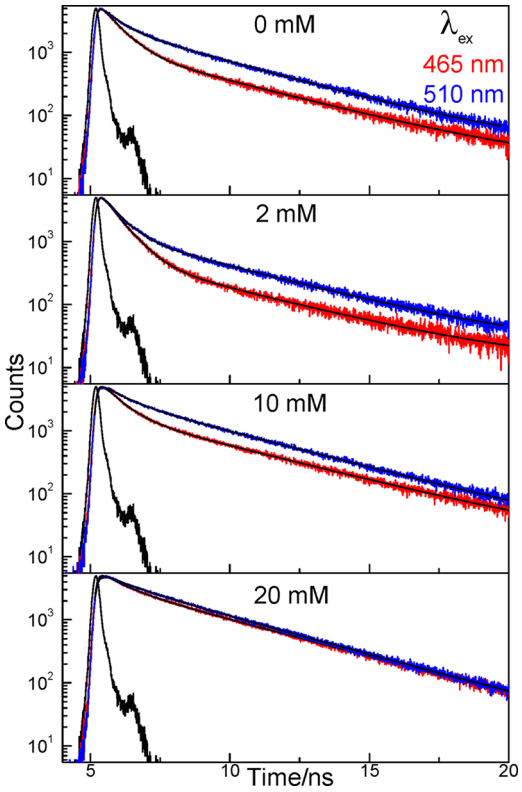

Figure 7. Fluorescence transients of $BP(OH)_2$ in 1% HSA with increasing SDS concentrations (0, 2, 10, and 20 mM) at two different emission wavelengths of 465 and 510 nm (λ_{ex} = 375 nm). The concentrations of SDS are specified in the plots.

CONCLUSION

The excited-state proton-transfer dynamics of $BP(OH)_2$ can be modulated in organized assemblies like micelles[19] and cyclodextrins.[31] This article reports the use of $BP(OH)_2$ as a fluorophore to investigate protein−surfactant interaction using steady-state and time-resolved spectroscopy. SDS with a negative interface is known[19] to promote the formation of the monocation of $BP(OH)_2$. In contrast, in protein−SDS aggregates the negative interface of SDS being shielded by the albumin chain retards the formation of the monocation. An early release of the fluorophores into the aqueous solution due to competitive binding of SDS at high-energy sites of the protein until 2 mM SDS concentration is observed in both steady-state and time-resolved studies. Massive cooperative binding of SDS upon denaturation of protein enhances the extent of ESIDPT owing to the stabilization of the diketo tautomer. This is certified by an increase in the quantum yield and radiative lifetime of the nonpolar diketo tautomer upon solubilization in these rigid aggregates. Formation of normal micelles beyond saturation leads to a spectral and temporal behavior similar as observed in SDS micelles reported earlier.[19] Thus, our observations and findings bolster the necklace and bead model. Furthermore, the unique ability of $BP(OH)_2$ to sense the polarity and rigidity of the system makes it a suitable fluorescent probe for the identification of the nature of heterogeneity in various organized assemblies and signifies its importance in biological applications.

ASSOCIATED CONTENT

Supporting Information

Additional fluorescence spectra, time-resolved decays, and table of decay parameters. This material is available free of charge via the Internet at http://pubs.acs.org.

AUTHOR INFORMATION

Corresponding Author

*Phone: +91 22 2576 7149. Fax: +91 22 2570 3480. E-mail: anindya@chem.iitb.ac.in.

Notes

The authors declare no competing financial interest.

ACKNOWLEDGMENTS

This work is supported by the SERC, DST. D.D. thanks CSIR for a Senior Research Fellowship.

REFERENCES

(1) Sukul, D.; Pal, S. K.; Mandal, D.; Sen, S.; Bhattacharyya, K. *J. Phys. Chem. B* **2000**, *104*, 6128−6132.
(2) Hassler, N.; Baurecht, D.; Reiter, G.; Fringeli, U. P. *J. Phys. Chem. C* **2011**, *115*, 1064−1072.
(3) Nörenberg, R.; Klinger, J.; Horn, D. *Angew. Chem., Int. Ed.* **1999**, *38*, 1626−1629.
(4) Jones, M. N. *Chem. Soc. Rev.* **1992**, *21*, 127−136.
(5) Yang, J. T.; Foster, J. F. *J. Am. Chem. Soc.* **1953**, *75*, 5560−5567.
(6) Reynolds, J. A.; Tanford, C. *Proc. Natl. Acad. Sci. U.S.A.* **1970**, *66*, 1002−1007.
(7) Steinhardt, J.; Krijn, J.; Leidy, J. G. *Biochemistry* **1971**, *10*, 4005−4015.
(8) Moriyama, Y.; Ohta, D.; Hachiya, K.; Mitsui, Y.; Tekeda, K. *J. Protein Chem.* **1996**, *15*, 265−272.
(9) Ding, F.; Li, X.-N.; Diao, J.-X.; Sun., Y.; Zhang, L.; Sun, Y. *Chirality* **2012**, *24*, 471−480.
(10) Otzen, D. *Biochim. Biophys. Acta* **2011**, *1814*, 562−591.
(11) Mukherjee, T. K.; Lahiri, P.; Datta, A. *Chem. Phys. Lett.* **2007**, *438*, 218−223.
(12) Gelamo, E. L.; Tabak, M. *Spectrochim. Acta, Part A* **2000**, *56*, 2255−2271.
(13) Gelamo, E. L.; Silva, C. H. T. P.; Imasato, H.; Tabak, M. *Biochim. Biophys. Acta* **2002**, *1594*, 84−99.
(14) Turro, N. J.; Lei, X.-G. *Langmuir* **1995**, *11*, 2525−2533.
(15) Chakraborty, A.; Seth., D.; Setua, P.; Sarkar, N. *J. Phys. Chem. B* **2006**, *110*, 16607−16617.
(16) Sahu, K.; Roy, D.; Mondal, S. K.; Karmakar, R.; Bhattacharyya, K. *Chem. Phys. Lett.* **2005**, *404*, 341−345.
(17) Chandar, P.; Somasundaran, P.; Turro, N. J. *Macromolecules* **1988**, *21*, 950−953.
(18) Vasilescu, M.; Angelescu, D.; Almgren, M.; Valstar, A. *Langmuir* **1999**, *15*, 2635−2643.
(19) De, D.; Datta, A. *J. Phys. Chem. B* **2011**, *115*, 1032−1037.
(20) Bulska, H. *Chem. Phys. Lett.* **1983**, *98*, 398−402.
(21) Lipkowski, J.; Grabowska, A.; Waluk, J.; Calestani, G.; Hess, B. A., Jr. *J. Crystallogr. Spectrosc. Res.* **1992**, *22*, 563−572.
(22) Bulska, H.; Grabowska, A.; Grabowski, Z. R. *J. Lumin.* **1986**, *35*, 189−197.
(23) Prosposito, P.; Marks, D.; Zhang, H.; Glasbeek, M. *J. Phys. Chem. A* **1998**, *102*, 8894−8902.
(24) Neuwahl, F. V. R.; Foggi, P.; Brown, R. G. *Chem. Phys. Lett.* **2000**, *319*, 157−163.
(25) Marks, D.; Prosposito, P.; Zhang, H.; Glasbeek, M. *Chem. Phys. Lett.* **1998**, *289*, 535−540.
(26) Zhang, H.; van der Meulen, P.; Glasbeek, M. *Chem. Phys. Lett.* **1996**, *253*, 97−102.
(27) Toele, P.; Zhang, H.; Glasbeek, M. *J. Phys. Chem. A* **2002**, *106*, 3651−3658.

(28) Sepoil, J.; Bulska, H.; Grabowska, A. *Chem. Phys. Lett.* **1987**, *140*, 607−610.
(29) Suresh, M.; Jose, D. A.; Das, A. *Org. Lett.* **2007**, *9*, 441−444.
(30) Kaczmarek, L.; Borowicz, P.; Grabowska, A. *J. Photochem. Photobiol., A* **2001**, *138*, 159−166.
(31) Abou-Zied, O. K. *J. Phys. Chem. B* **2007**, *111*, 9879−9885.
(32) Abou-Zied, O. K. *J. Phys. Chem. B* **2010**, *114*, 1069−1076.
(33) Abou-Zied, O. K.; Al-Hinai, A. T. *J. Phys. Chem. A* **2006**, *110*, 7835−7840.
(34) Rurack, K.; Hoffmann, K.; Al-Soufi, W.; Resch-Genger, U. *J. Phys. Chem. B* **2002**, *106*, 9744−9752.
(35) Abou-Zied, O. K. *J. Photochem. Photobiol., A* **2006**, *182*, 192−201.
(36) Enchev, V. *Int. J. Quantum Chem.* **1996**, *57*, 721−728.
(37) Carballeira, L.; Perez-Juste, I. *J. Mol. Struct. (THEOCHEM)* **1996**, *368*, 17−25.
(38) Wortmann, R.; Elich, K.; Lebus, S.; Liptay, W.; Borowicz, P.; Grabowska, A. *J. Phys. Chem.* **1992**, *96*, 9724−9730.
(39) Melhuish, W. H. *J. Phys. Chem.* **1961**, *65*, 229−235.
(40) Mukherjee, T. K.; Panda, D.; Datta, A. *J. Phys. Chem. B* **2005**, *109*, 18895−18901.
(41) Mishra, P. P.; Koner, A. L.; Datta, A. *Chem. Phys. Lett.* **2004**, *400*, 128−132.
(42) Haldar, A.; Sen, P.; Burman, A. D.; Bhattacharyya, K. *Langmuir* **2004**, *20*, 653−657.